Reorganization in cerebral and cerebellar cortices is not restricted by proximity between body-part representations

Abbreviated title: Somatotopy does not limit reorganization

Avital Hahamy[1,2] and Tamar R. Makin[3]

[1]Wellcome Trust Centre for Neuroimaging, UCL Queen Square Institute of Neurology, University College London, 12 Queen Square, London WC1N 3AR, UK.

[2]Department of Neurobiology, Weizmann Institute of Science, Rehovot, Israel.

[3]Institute of Cognitive Neuroscience, University College London, 17 Queen Square, London WC1N 3AZ, UK.

Corresponding author:

Avital Hahamy, Email: avital.hahamy@gmail.com

Conflict of Interests: The authors declare no competing financial interests

Acknowledgements:

We thank Alona Cramer, Jan Scholtz, Fiona van der Heiligenberg, Harriet Dempsey Jones and Lucilla Cardinali for help in data collection, and Victoria Root for helpful comments on the manuscript. We thank Opcare for help with recruitment, and our participants for taking part in these studies.

Abstract

Different terminals of the sensorimotor network show varied somatotopic arrangements of body-part representations. Since somatotopy is best characterized in the primary somatosensory (S1) and motor (M1) cortices, these terminals have been the main target for research on somatotopic alterations following loss of sensory input (e.g. arm amputation). Such reorganization is generally considered to be driven by the spatial layout of the underlying somatotopy, such that neighboring body-part representations tend to occupy the deprived brain region. For example, following arm deafferentation in non-human primates, the S1 deprived hand area becomes responsive to inputs from the chin, which has a native representation that cortically neighbors that of the (now deprived) hand region. Here we challenge the assumption of proximity-based reorganization, by comparing patterns of reorganization in the cerebellum and the primary sensorimotor cortex, in several independently acquired datasets of people born without one hand (hereafter, one-handers) and two handed controls. Based on this internal replication, we demonstrate that in the cerebellum of one-handers, the deprived hand region represents multiple body-parts, despite varying distances between the native representations of these body-parts and the deprived hand region. We further replicate our previously reported finding, showing a similar pattern of reorganization in the deprived hand region of the cerebral cortex in one-handers. Since the cerebellar and cerebral cortices contain different somatotopic layouts, the parallel reorganization observed in these two terminals demonstrates that the mere spatial layout of body-part representations may not exclusively dictate reorganization in the sensorimotor network. Instead, we discuss alternative drivers of reorganization, and particularly, the possible role of adaptive behavior and sub-cortical plasticity.

Significance Statement

When a hand is missing, the brain region that typically processes information from that hand may instead process information from other body-parts, a phenomenon termed reorganization. It is commonly thought that only body-parts whose information is processed in regions adjacent to the hand region, could take up the resources of this now deprived region. Here we demonstrate that information from the same body-parts is processed in the hand regions of both the cerebral cortex and cerebellum. The native brain regions of these body-parts have varied relative distances from the hand region of the cerebellum compared to the cerebral cortex, and do not necessarily neighbor these hand regions. We therefore propose that proximity between brain regions cannot fully explain brain reorganization.

Introduction

The “sensorimotor homunculus” in primary somatosensory and motor cortices is thought to reflect the lateralized and segregated neural activation patterns associated with sensations from- and movements of-distinct body parts (Penfield and Boldrey, 1937; Penfield and Rasmussen, 1950; Catani, 2017; Roux et al., 2018). Following input and output loss, e.g. following arm amputation, the sensorimotor homunculus undergoes reorganization, such that the region previously responsible for representing the hand becomes responsive to inputs from other body-parts (Flor et al., 1995; Makin et al., 2013b; Chand and Jain, 2015; Raffin et al., 2016). The organizing principles underlying such architectural change are thought to derive from the spatial layout of the homunculus: neighboring representations, which share greater cortical overlap (Merzenich et al., 1984; Pons et al., 1991; Merzenich and Jenkins, 1993; Florence et al., 1998) and/or receive stronger inhibition from now absent inputs (Faggin et al., 1997; Margolis et al., 2012) are more likely to “invade” the deprived cortical region. Subsequently, findings showing increased expression of facial inputs in the missing-hand region following arm amputation have been taken as evidence for the role of somatotopic layout in scaffolding reorganization (Jain et al., 2008; Kaas et al., 2008; MacIver et al., 2008; Foell et al., 2014; Andoh et al., 2017).

We and others have recently challenged this view, by demonstrating that reorganization may also occur between distal body-part representations. For example, the intact hand of amputees shows increased representation in the region of the missing hand in the primary sensorimotor cortex (hereafter deprived cerebral hand region) (Bogdanov et al., 2012; Makin et al., 2013b; Philip and Frey, 2014). Similarly, individuals with bilateral hand-loss show increased feet representation in their deprived cerebral hand region (Stoeckel et al., 2009; Yu et al., 2014; Striem-Amit et al., 2018). This feet-to-hand reorganization occurs despite the inherent cortical distance between feet and hand representations. Finally, in individuals born without one hand (hereafter, one-handers) multiple body parts (residual arm, lips and feet , but not the intact hand) show increased representation in the deprived cerebral hand region (Makin et al., 2013b; Hahamy et al., 2017). As the representations of the feet and lips are not the immediate neighbors of the

hand region, we have suggested that proximity between body-part representations is not a prerequisite for reorganization. Yet, it has recently been argued that reorganization in the hand regions of people born without two hands is mostly restricted to neighboring body parts representations (Striem-Amit et al., 2018). Thus, proximity between body-part representations is still considered the main driver of reorganization in both congenital and late-onset sensorimotor deprivation.

Here we address this question by examining reorganization in one-handers, at multiple sensorimotor terminals with varying somatotopic arrangements. Somatotopic organization has been previously identified throughout the sensorimotor network, such as in the cerebellum (Manni and Petrosini, 2004), brainstem (Jang et al., 2011), basal ganglia and motor thalamus (Nambu, 2011). Since somatotopic representations in the human cerebellum can be reliably identified using fMRI (Grodd et al., 2001; Buckner et al., 2011; Wiestler et al., 2011; Haak et al., 2017), we use the cerebellum as a model for examining the role of somatotopic layout in shaping sensorimotor brain reorganization in one-handers. The organization of body-part representations in the cerebellum differs from that of the primary sensorimotor homunculus (Manni and Petrosini, 2004; Mottolese et al., 2013; Mottolese et al., 2015), allowing us to study whether differences in the spatial layout of representations would lead to different patterns of reorganization between the cerebral and cerebellar deprived hand regions. Here, we address this question using several independently-acquired datasets of one-handers and two-handed controls. By meta-analyzing the results of these datasets we provide robust evidence that the same body-part representations (residual arm, lips and feet) are remapped to the deprived hand region of the cerebellar and cerebral cortices, thus documenting similar large-scale reorganization across the hierarchy of the sensorimotor network. We therefore propose that reorganization is not determined by the physical proximity between the native and remapped representations, and discuss alternative factors that may underlie this extensive brain plasticity.

Materials and Methods

Participants

This study makes use of three independently acquired fMRI datasets of one-handers and two-handed controls. Two of these datasets had cerebellar coverage, and were therefore used for cerebellar analyses. All three datasets were used for analysis of the cerebral cortex (note that cerebral cortex findings in the third dataset have been published in Hahamy et al., 2017).

Recruitment was carried out in accordance with NHS national research ethics service approval (10/H0707/29, dataset1) and with Oxford University's Medical Sciences inter-divisional research ethics committee (MS-IDREC-C2- 2015-012, dataset2). Informed consent and consent to publish was obtained in accordance with ethical standards set out by the Declaration of Helsinki.

The first dataset (hereafter, Dataset1) contains the same population recruited for a previous study, using the same scanning procedures and exclusion criteria as described before (Hahamy et al., 2015b). 25 healthy controls (15 females, age = 41.12±12.86, 8 left hand dominant) and 14 individuals with a congenital unilateral upper limb deficit (one-handers, 9 females, age = 36.64±12.02, 4 with absent right hand) were recruited for the study. The proportion of one-handers with a missing right hand (n=4) and controls who are left-hand dominant (n=8) were similar ($\chi^2_{(1)}$=0.18, p=0.67).

The second dataset (hereafter, Dataset2) was acquired as part of a larger study (the full study protocol is currently under preparation and will be made available via Open Science Framework). These data include the scanning of 12 healthy controls (5 females, age = 45.33±14.85, 5 left hand dominant), and 14 one-handers (7 females, age = 45.25±11.38, 6 with absent right hand) (see Table 1 for demographic details). The proportions of one-handers with a missing right hand (n=6) and controls who are left-hand dominant (n=5) were similar ($\chi^2_{(1)}$=0.05, p=0.82). Four one-handers participated in both studies, with data acquired some 5 years apart.

Full demographic description and acquisition-related information regarding the third dataset is available in Hahamy et al., 2017.

Experimental Design

Scanning protocol for both datasets included multiple scans (see protocol in https://osf.io/4vcmx/). Only an anatomical T1 scan and a task scan for body-part functional localization were used and analyzed here (these scanning procedures were described previously, see Makin et al., 2013b; Hahamy et al., 2015b).

The sensorimotor task in both datasets followed the same procedure: Participants were visually instructed to move each of their hands (finger flexion/extension), arms (elbow flexion/extension), their feet (bilateral toe movements), or lips, as paced by a visual cue. Note that none of the one-handers experienced phantom sensations. Therefore, in conditions concerning missing hand movements (and elbow movements for one participant with an above-elbow deficiency) participants were instructed to imagine moving their missing limb. This condition was only included to match the experimental design across groups and was not submitted to statistical analyses. The protocol consisted of alternating 12-s periods of movement and rest. Each of the six conditions was repeated four times in a semi-counterbalanced order. Participants were trained before the scan on the degree and form of the movements. To confirm that appropriate movements were made at the instructed times, task performance was visually monitored online, and video recordings were made in a subset of the scans for further off-line evaluation.

MRI data acquisition

The MRI measurements of Dataset1 were obtained using a 3T Verio scanner (Siemens, Erlangen, Germany) with a 32-channel head coil. Anatomical data were acquired using a T1-weighted magnetization prepared rapid acquisition gradient echo sequence (MPRAGE) with the parameters: TR: 2040 ms; TE: 4.7 ms; flip angle: 8°, voxel size: 1 mm isotropic resolution. Functional data based on the blood oxygenation level-dependent (BOLD) signal were acquired using a multiple gradient echo-planar T2*-weighted pulse sequence, with the parameters: TR: 2000 ms; TE: 30 ms; flip angle: 90°; imaging

matrix: 64 × 64; FOV: 192 mm axial slices. 46 slices with slice thickness of 3 mm and no gap were oriented in the oblique axial plane, covering the whole cortex, with partial coverage of the cerebellum.

MRI images of Dataset2 were acquired using a 3T MAGNETON Prisma MRI scanner (Siemens, Erlangen, Germany) with a 32-channel head coil. Anatomical images were acquired using a T1-weighted sequence with the parameters TR: 1900 ms, TE: 3.97 ms, flip angle: 8°, voxel size: 1 mm isotropic resolution. Functional images were collected using a multiband T2*-weighted pulse sequence with a between-slice acceleration factor of 4 and no in-slice acceleration. This allowed acquiring data with increased spatial (2mm isotropic) and temporal (TR: 1500ms) resolution, covering the entire brain. The following acquisition parameters were used - TE: 32.40ms; flip angle: 75°, 72 transversal slices. Field maps were acquired for field unwarping.

Preprocessing of functional data

All imaging data were processed using FSL 5.1 (www.fmrib.ox.ac.uk/fsl). Data collected for individuals with absent right limbs were mirror reversed across the mid-sagittal plane prior to all analyses so that the hemisphere corresponding to the missing hand was consistently aligned. Data collected for left-hand dominant controls were also flipped, in order to account for potential biases stemming from this procedure. Note that the proportion of flipped data did not differ between experimental groups in either datasets ($\chi^2_{(1)}$=0.18, p=0.67 for Dataset1; $\chi^2_{(1)}$=0.05, p=0.82 for Dataset2), and that this flipping procedure has been validated using multiple approaches (see Hahamy et al., 2017).

Functional data were analyzed using FMRIB's expert analysis tool (FEAT, version 5.98). The following pre-statistics processing was applied to each individual task-based run: motion correction using FMRIB's Linear Image Registration Tool (Jenkinson et al., 2002); brain-extraction using BET (Smith, 2002); mean-based intensity normalization; high pass temporal filtering of 100 s; and spatial smoothing using a Gaussian kernel of FWHM (full width at half maximum) 4 mm. Time-course statistical analysis was carried out using FILM (FMRIB's Improved Linear Model) with local autocorrelation correction. Functional data were aligned to structural images (within-subject) initially using linear registration

(FMRIB's Linear Image Registration Tool, FLIRT), then optimized using Boundary-Based Registration (Greve and Fischl, 2009). Structural images were transformed to standard MNI space using a non-linear registration tool (FNIRT), and the resulting warp fields were applied to the functional statistical summary images.

Statistical analyses

Meta-analysis approach

The current study makes use of three separate datasets, acquired across several years and using different magnets and scanning parameters. Two of these datasets included coverage of the cerebellum and were therefore used for cerebellar analysis, and all thress datasets were used for analysis of the cerebral cortex. Multiple datasets can, in principle, be collapsed for analysis purposes, benefiting statistical power to identify weak effects that may not be noticeable in each separate dataset (Friston, 2012). However, as the current study is guided by an a-priori hypothesis that is also spatially focal (reorganization in the deprived hand region of one-handers), it calls for more stringent inference methods rather than for exploratory ones that benefit from enhanced power. We therefore opted to analyzing each dataset separately and combining results using a meta-analysis approach, which allowed us to test inherent reproducibility of findings across datasets, and hence make more valid inferences (Ioannidis et al., 2014; Picciotto, 2018).

Our analysis pipeline for all ROI-based analyses reported below included a-parametric permutation tests performed within each separate dataset. Note that permutation tests are statistically stringent as they make no assumptions regarding the finite sample distribution of the data, but rather derives it given the data observed (Holmes et al., 1996; Nichols and Holmes, 2002), and are also less sensitive to outlier effects (Masyn et al., 2013), thus contributing to the robustness of findings. The dataset–specific p-values resulting from each of the below-described permutation tests were then combined across datasets and meta-analyzed using Fisher's method (Fisher, 1925; Fisher, 1948) to test the reproducibility of results across datasets. To establish the robustness of the reported effects, p-values were additionally tested using Stouffer's test (Stouffer et al., 1949) and the weighted Z-test (weights set to

the square root of each sample size, Liptak, 1958). To correct for multiple hypotheses testing across the 3 experimental conditions of interest (movements of the residual arm, lips and feet), the alpha level was adjusted to 0.017 based on the highly conservative Bonferroni correction.

Whole-brain analysis

All statistical analyses were designed to follow the procedures described in our original report (Hahamy et al., 2017). Statistical analyses were conducted using FSL and in-house Matlab code. To compute task-based statistical parametric maps, we applied a voxel-based general linear model (GLM), as implemented in FEAT, using a double-gamma hemodynamic response function and its temporal derivative convolved with the experimental model. The 6 motion parameters and their derivatives were also included in the GLM as nuisance regressors. Our main comparisons contrasted intact/dominant hand, residual/nondominant arm, lips and feet conditions against a baseline (rest) condition.

Group level analysis of statistical maps was carried out using FMRIB's Local Analysis of Mixed Effects (FLAME). Intact hand movements in the one-handed group were compared with dominant hand movements in controls, and residual arm movements were compared with non-dominant arm movements. The cross-subject GLM included planned comparisons between the two groups. Z (Gaussianized T/F) statistic images were thresholded using clusters determined by $Z>2.6$ ($p<0.01$), and a family-wise-error corrected cluster significance threshold of $p<0.01$ was applied to the suprathreshold clusters. Note that this whole-brain analysis tests the specificity of plasticity to the deprived hand region of one-handers, hence a lenient statistical threshold ($p<0.05$) is typically used in such procedures (Makin et al., 2013b; Hahamy et al., 2017). Nevertheless, as we test several whole-brain comparisons (residual arm, lips, feet conditions), we chose a more strict threshold of 0.01 across our tests to correct for any alpha inflation.

For visualization purposes only, condition-specific group maps were created for both the cerebellum and cerebral cortex, using the same statistical procedure reported above. These maps were merely aimed to visualize the sources of the reported group-differences, and hence were presented at varying thresholds that best capture the effects observed in the direct statistical comparisons between

groups. Under the same rationale, maps were presented before correction for multiple comparison, to best visualize group differences.

For presentation purposes, statistical parametric activation maps of the cerebellum were projected onto a flat cerebellar surface using SUIT (Diedrichsen and Zotow, 2015), and parametric activations in the cerebral cortex were projected onto an inflated cortical surface of a representative participant's cortex using workbench.

Cerebellar Regions Of Interest (ROI) definition

In order to ascertain that the observed increased cerebellar activation in one-handers (observed across the two datasets with cerebellar coverage) falls within the hand region, and to measure its extent, single-subject activation values were extracted from independently defined hand-region ROIs and compared between experimental groups. To define the cerebellar hand regions of the dominant/intact hemisphere (contralateral to the dominant/intact hand) and nondominant/deprived hemisphere (ipsilateral to the dominant/intact hand), the 100 cerebellar voxels of highest activation evoked by either dominant or nondominant hand movements in the control group of one dataset were used as ROIs in the second dataset, and vice-versa (see Table 2, Figures 1,3). Percent signal change activation values from the individual statistical parametric maps were extracted for the intact and deprived hand ROIs for each participant in the residual/nondominant arm, lips, feet and intact hand conditions. Since the functional data of one control participant in Dataset1 did not cover the cerebellum, data from this individual were excluded from the cerebellar ROI analysis. The same method was used to define the cerebellar representation of the lips and feet for visualization purposes.

Statistical analysis of cerebellar ROIs

To a-parametrically assess each planned group-contrast (experimental conditions involving movements of different body parts), permutation tests were employed within each dataset separately (Holmes et al., 1996; Nichols and Holmes, 2002). In each experimental condition separately, the test statistic was set as the difference between mean group activations in a certain ROI. Next, participants' labels (one-handers or

control) were permuted under the null hypothesis of no group differences in the levels of ROI activation under each experimental condition. Thus, two random experimental groups were created for each condition, and the difference between the groups' mean activation in a given ROI was calculated. This procedure was repeated 10,000 times, creating 10,000 random differences that constructed the null distribution. For each experimental condition, the position of the true (unshuffled) group-difference relative to the null distribution was used to obtain a two-sided p-values. Using the same pipeline, under the null hypothesis of no 2-way interactions between groups and hemispheres (ipsilateral and contralateral to the missing/nondominant hand), both participants' labels and within-participant hemisphere-labels were permuted in each dataset and experimental condition separately. The differences between hemisphere-scores were calculated per participant, averaged across participants of the same experimental group, and mean group differences were derived. The position of the true group-difference relative to the null distribution (resulting from 10,000 such iterations) in each experimental condition was used to derive a two-sided p-value.

Assessing reorganization in the cerebral cortex

The overlap in participants between Datasets1 and Datase2 is relatively small (4 out of 24 participants), which allowed us to perform the above described cross-dataset replication analyses for the cerebellum. However, we also aimed to test the reproducibility of our previously reported findings of reorganization in the cerebral cortex (Hahamy et al., 2017) using the two current datasets and a previously published dataset, and these contained larger overlap in participants. Dataset2 included only 5 participants who also participated in the Hahamy et al., 2017 study (with data acquired some 2 years apart). However Dataset1 and the data used in Hahamy et al., 2017 greatly overlapped (12 out of 14 participants, with data acquired some 3 years apart). Hence, cerebral-related results obtained from Dataset1 should be taken as a measure of test-retest reliability with regards to Hahamy et al., 2017, rather than an independent replication.

Analyses performed on the cerebral cortex are identical to those described for the cerebellum, except for the following differences: 1) For cerebral hand ROIs (in both hemispheres) we used

independent regions previously defined based on the original sample of one-handers and controls of our previous study (Hahamy et al., 2017; see Table 2; this ROI will be made freely available via open science framework), to standardize the analysis across the three datasets (the two current ones and the previously published one). ROIs for lips and feet sensorimotor representations were also adopted from the same previous work to visualize the sensorimotor homunculus. Note that limitations in both MRI acquisition and analysis resolution precluded reliable separation between the two cerebral foot regions. For this reason, a bilateral ROI was defined for the feet. For the same technical reasons we were unable to dissociate the somatosensory and motor primary cortices (SI and M1, respectively). Therefore, all body part ROIs are labelled 'sensorimotor'. 2) Since the cerebral-focused ROI analyses were guided by a predefined hypothesis (over-representation of the residual arm, lips and feet in the deprived hand region of one-handers) based on our previous study, one-tailed statistical tests within each of Dataset1 and Dataset2 were used. Since our previous study did not find a significant interaction between groups and hemispheres for the feet condition, the tests of this effect in the two current datasets were performed in a two-tailed form. For each experimental condition, sets of 3 dataset-specific p-values (resulting from each of the two current datasets, as well as the previously reported p-values of the original dataset) were combined and tested using the same methods described for the cerebellum analyses, including correction for multiple comparisons.

Assessing reorganization in the putamen

Reorganization in the putamen was studied using a more exploratory approach compared to the approach employed for the study of the cerebellum and cerebral cortex. The deprived and intact putamen ROIs were defined based on the Harvard-Oxford probabilistic atlas, at a probabilistic threshold of 90 (see Table 2). Activations in these ROIs were compared between the experimental groups of Dataset2 alone (which had better spatial resolution, allowing the study of small subcortical structures), using two-sided permutation tests, as described for the cerebellar ROI analyses.

Confirmatory analysis: spatial layout of body-part representations

To measure cortical proximity between native body-part representations, the level of overlap between activations of the hand, lips and feet in the "intact" hemisphere (cerebral hemisphere contralateral to the dominant/intact hand and cerebellar hemisphere ipsilateral to the dominant/intact hand) were measured in all participants using the Dice coefficient (Dice, 1945; Kikkert et al., 2016):

$$\frac{2 \times |A \cap B|}{|A| + |B|}$$

Where A and B represent activation evoked by movements of specific body-parts (intact hand and lips or intact hand and feet) within a sensorimotor mask. To that end, for each participant, the activation maps of intact hand, lips and feet conditions were minimally thresholded at z=2 to allow a relatively wide spread of activation. The few participants who had particularly low spread of activation (<25 voxels) in the intact hemisphere in either condition, despite the lenient threshold, were excluded from this analysis (Dataset1: 3 control participants; Dataset2: one congenital and one control participant). In the cerebral cortex, the level of overlapping activations between the hand condition and each of the lips and feet conditions were assessed within a mask of the left pre-central gyrus, taken from the Harvard-Oxford probabilistic atlas (this mask was used unthresholded to contain the central sulcus and both the pre- and post-central gyri, see Figure 9A). In the cerebellar cortex, the level of overlapping activations between the hand condition and each of the lips and feet conditions were assessed within a mask of right lobules I-IV,V and VI, taken from FSL's cerebellar probabilistic atlas. Each of these three cerebellar masks were thresholded at 50 prior to their unification in order to restrict the unified mask to the sensorimotor sections of the cerebellar anterior lobe (see Figure 9A).

For each participant, 4 Dice coefficients were calculated: overlap between intact hand and feet activations, and overlap between intact hand and lips activations, in each of the cerebrum/cerebellum masks separately. We next aimed to verify that the overlap relationship of body-part representations differs between the cerebrum and the cerebellum, as previously reported (see Introduction). However, a direct comparison between overlap in representations in the cerebrum vs. cerebellum may be confounded by the different spatial scales of these two structures. We therefore targeted a comparison between intra-

structure overlap relations, which we will refer to as "neighborhood relationship" of each of the cerebral or cerebellar cortices. This neighborhood relationship was defined as the ratio of lips-hand overlap to feet-hand overlap in each brain structure (cerebrum/cerebellum, Figure 9C). Note that as neighborhood relationships are devised as ratios within each brain structure, they normalize the Dice coefficients and enable a comparison between the cerebrum and cerebellum. To evaluate whether these neighborhood relationships are different between the cerebrum and cerebellum, a permutation test was employed within each dataset. The test's statistic was defined as the cross-participants mean ratio between cerebellar neighborhood relationship and cerebral neighborhood relationship (a ratio that significantly deviates from 1 would suggest a difference in topographies between the cerebrum and cerebellum). To this end, for each participant, the cerebral neighborhood relationship was divided by the cerebellar neighborhood relationship. Under the null hypothesis of no difference between cerebral and cerebellar neighborhood relationships, the cerebral and cerebellar neighborhood relationships were shuffled within participants and then averaged across participants, a procedure which was repeated 10,000 times to create the null distribution. The position of the true (unshuffled) test statistic within this distribution was then used to obtain a two-sided p-value. Finally, the resulting dataset-specific p-values were tested using Fisher's method to assess the consistency of affects across datasets.

Results

Cerebellar reorganization is not restricted by somatotopic layout

To test whether somatotopy restricts reorganization in the cerebellum, we assessed functional reorganization of the residual arm (overlapping the hand area, Figure2), as well as the lips and feet (whose representations have differing levels of overlap with the hand area) in one-handers compared to controls. To this end, we compared results across two independently acquired datasets of one-handers and controls who underwent a functional MRI scan, involving simple movements of hands, arms, lips and feet. Whole-brain activations evoked by movements of the residual/nondominant arm, lips and feet (body-

part representations previously shown to reorganize in the cerebral cortex, Hahamy et al., 2017), and of the intact hand (whose representation did not show such reorganization, Hahamy et al., 2017) was compared between experimental groups within each dataset. These analyses revealed that movements of the lips and feet, but not movements of the intact hand, excessively activated a region in Lobules V \ VI of the cerebellar hemisphere ipsilateral to the missing hand in one-handers (see Figures 1,3, Table 3). These clusters overlapped with the independently defined ROI of the deprived hand region of the anterior cerebellum (see Materials and Methods, Figure 1). Unlike our previous findings in the cerebral cortex, this whole-brain group contrast did not reveal increased activation in one-handers for residual arm movements compared to controls. This could potentially stem from near complete overlap between the arm and hand representations found in the cerebellum (Mottolese et al., 2013, and see Figure 2). Specifically, if the arm representation naturally overlaps with the hand representation, additional remapping between these representations in one-handers may be too subtle to be detected using a whole-brain analysis. Additional clusters showing increased activation in one-handers compared to controls were also found within specific datasets, but unlike the deprived hand region, these clusters were not consistent across all datasets and task-conditions (see Table 4). The results of the direct grop-contrasts were further visualized using group activation maps of each condition vs. rest (Figure 3).

We next aimed to measure the degree of remapped activation in the deprived cerebellar hand region during movements of different body parts, and assess its consistency across datasets. To this end, within each dataset and movement condition separately, between-group permutation tests were used to compare mean fMRI activation values (percent signal change) obtained from two independent hand ROIs (deprived and intact hand regions of the cerebellar hemispheres' anterior lobe, ROIs depicted in Figures 1,3). These ROIs were obtained from the control group of one dataset and tested on the other dataset, and are completely independent of the group-contrast activations reported above. Results of these tests were combined across the two datasets (See Materials and Methods; Dataset-specific p-values for all experimental conditions are presented in Table 5). These analyses confirmed increased activation in the deprived cerebellar hand ROI when one-handers moved their lips ($\chi^2_{(4)}$=23.21, $p<0.001$, $\alpha=0.017$

Bonferroni corrected, Fisher's test) and feet ($\chi^2_{(4)}$=19.91, p<0.001, α=0.017 Bonferroni corrected, Fisher's test), as well as their residual arm ($\chi^2_{(4)}$=15.29, p=0.004, α=0.017 Bonferroni corrected, Fisher's test), compared with controls. Movements of the intact hand (whose representation does not reorganize in the cerebral cortex, Hahamy et al., 2017) did not result in increased representation in the deprived cerebellar hand region of one-handers ($\chi^2_{(4)}$=3.33, p=0.51, Fisher's test). In addition, two-way interactions were consistently revealed between hemispheres and groups (non-dominant/residual arm: $\chi^2_{(4)}$=20.61, p<0.001; lips: $\chi^2_{(4)}$=19.39, p<0.001; feet: $\chi^2_{(4)}$=19.23, p<0.001, Fisher's test, α=0.017 Bonferroni corrected for all tests). These interactions reflect dissociated recruitment of the deprived cerebellar hand region by movements of various body parts in one-handers, in comparison with the intact cerebellar hand region and with the control group, as shown in the Figure 4. These findings echo the pattern of reorganization we previously reported in the cerebral cortex of one-handers, and reflect sensorimotor reorganization which is not restricted by the topographic arrangement of representations in the cerebellar homunculus.

Similar pattern of reorganization seen in the cerebellar and cerebral deprived hand regions of one-handers

We next used these two datasets to test the reproducibility of our previous findings of reorganization in the cerebral cortex of one-handers (our previously reported results were based on Dataset3, and can be found in Hahamy et al., 2017). As shown in Figure 5 (and further visualized in Figure 6), movements of the residual arm, lips or feet, but not movements of the intact hand, activated the sensorimotor cerebral cortex to a greater extent in one-handers compared to controls, as shown using whole-brain contrast maps. For all three body parts, increased activation in one-handers was centered on the hand knob of the central sulcus in the deprived hemisphere, spanning both the pre- and post-central gyrus of the hemisphere contralateral to the missing hand (see Table 3). These clusters overlapped with an ROI of the putative region of the missing hand in the cerebral cortex (see Materials and Methods, Figure 5). Additional clusters showing increased activation in one-handers compared to controls were also found within

specific datasets, but unlike the deprived hand region, these clusters were not consistent across all datasets and task-conditions (see Table 4).

Next, an ROI analysis of the cerebral hand regions was performed using independently defined ROIs (ROIs presented in Figures 5,6). These group-based ROIs, defined based on our previously analyzed dataset of participants (Hahamy et al., 2017), were used to preserve consistency with our previous study and allowed us to combine results across the two current datasets as well as the dataset used in our previous study to assess reproducibility (dataset-specific p-values for all experimental conditions are presented in Table 5). As depicted in Figure 7, these tests confirmed increased activation in the deprived cerebral hand ROI when one-handers moved their residual arm ($\chi^2_{(6)}$=47.73, p<0.001, α=0.017 Bonferroni corrected, Fisher's test), lips ($\chi^2_{(6)}$=43.8, p<0.001, α=0.017 Bonferroni corrected, Fisher's test) and feet ($\chi^2_{(6)}$=37.08, p<0.001, α=0.017 Bonferroni corrected, Fisher's test) compared with controls. In addition, two-way interactions between hemispheres and groups consistently revealed dissociated recruitment of the deprived cerebral hand region (compared to the intact hand region) by movements of various body parts between one-handers and controls (non-dominant/residual arm: $\chi^2_{(6)}$=32.54, p<0.001; lips: $\chi^2_{(6)}$=28.07, p<0.001; feet: $\chi^2_{(6)}$=23.7, p<0.001, Fisher's test, α=0.017 Bonferroni corrected in all tests). Similar group differences were not found when participants were moving their intact/dominant hand ($\chi^2_{(6)}$=8.31, p=0.22, Fisher's test).

Table 6 presents the results of integration across datasets using additional meta-analysis measures for both the cerebral and cerebellar hand regions.

Reorganization in the Putamen

As indicated in Table 4, a whole-brain analysis of Dataset2 revealed that one-handers activated the deprived putamen to a greater degree compared to controls during lip movements. Though this effect was only seen in one dataset and one experimental condition, since the basal ganglia has reciprocal connections with both the cerebellum and the primary sensorimotor cortex (Nambu, 2011; Dum et al., 2014; Zeharia et al., 2015), we decided to follow up these results with more exploratory analyses. The left panel of Figure 8 depicts uncorrected group-contrast maps of Dataset2. Similar to our results in the

cerebellum and primary sensorimotor cortex, these maps demonstrated increased activation in the deprived putamen in the residual arm, lips and feet conditions, but not in the intact hand condition of one-handers compared to controls. Though only results of the lip condition survived correction for multiple comparisons, it is important to note that putamen fMRI activations, like those of other subcortical regions, are much noisier than those of the cerebrum and cerebellum. Since this region is also very small, relatively weak effects in this region are unlikely to survive correction for multiple comparisons in a whole-brain analysis.

A more sensitive test for reorganization in the putamen is therefore an ROI analysis. Indeed, as depicted in the right panel of Figure 8, these tests revealed significantly increased activation in the deprived putamen in the residual arm ($p=0.01$, permutation test), lip ($p=<0.001$, permutation test) and feet conditions ($p=0.02$, permutation test), but not in the intact hand condition ($p=0.1$, permutation test). These effects were accompanied by significant group (controls/one-handers) by hemisphere (intact/deprived putamen) interactions (residual arm: $p=0.048$, lip: $p=0.007$, feet: $p=0.057$, permutation tests), demonstrating the specificity of this effect to the deprived putamen. Note that, unlike in the cerebrum and cerebellum, activation in the putamen tends to be bilateral (Gerardin et al., 2003), hence the non-negligible activation levels in both hemispheres.

Confirmatory analysis: neighborhood relationship between body-part representations differ between the cerebrum and cerebellum

In both the cerebral and cerebellar cortices, the hand area resides between the foot and lip representations, however, the level of overlap between these representations was previously reported to differ between the two brain structures (see introduction). To verify this difference in overlap between body-part representations (hereafter, neighborhood relationship) in the cerebrum and cerebellum, we used brain activations as a proxy for representations.

To measure the extent of overlap between representations, we confined activations to the sensorimotor parts of the cerebellum and cerebrum (Figure 9A), and employed the Dice coefficients (Dice, 1945; Kikkert et al., 2016; see Materials and Methods). As demonstrated in the intact/dominant hemispheres of controls and one-handers in Figure 9B, some degree of overlap was indeed observed between the peripheral aspects of the hand region and the lip and feet activations of both cerebrum and cerebellum, allowing us to quantify overlapping activations within each brain structure. This level of overlap was evaluated using permutation tests on each of the dataset-specific Dice coefficients. Results of these tests were then combined across the two datasets (See Materials and Methods). This analysis demonstrated differences in neighborhood relationships between the cerebrum and cerebellum (Dataset1 $p=0.02$, Dataset2 $p=0.048$ permutation tests; Meta-analysis: $\chi^2_{(4)}=13.59$, $p=0.009$ Fisher's test, $\alpha=0.05$), reflecting that the representations of lips and feet in the cerebral cortex show more similar levels of overlap with the hand representation (Makin et al., 2015) relative to the cerebellum (Figure 9C).

Discussion

Here we report large scale neural reorganization of body-part representations in both the cerebellar and cerebral homunculi of individuals born without one hand. We previously demonstrated reorganization in the primary sensorimotor cortex, such that the residual arm, lips and feet, but not the intact hand, are simultaneously represented in the deprived cerebral hand region (Hahamy et al., 2017). Here we replicate these findings and extend them to the deprived hand region of the cerebellum. Of importance, in both the cerebellum and cerebrum, the representations of multiple body parts excessively expand into the deprived hand region (Figures 1 & 5). This expansion occurs despite differences in the somatotopic layout in these two sensorimotor terminals (Manni and Petrosini, 2004; Mottolese et al., 2013; Makin et al., 2015; Mottolese et al., 2015). Our findings therefore challenge the view that sensorimotor reorganization is restricted to the immediate neighbors of the deprived region (Merzenich et al., 1984; Pons et al., 1991; Merzenich and Jenkins, 1993; Faggin et al., 1997; Florence et al., 1998; Margolis et al., 2012).

Previous studies of similar sensorimotor-deprived populations have produced mixed evidence for the extent and drivers of reorganization. As such studies of reorganization rely on rare clinical populations, published results tend to be based on relatively small sample sizes, and replication of results is scarce. Here we constructed the largest imaging database to date of one-handers (n=26), and demonstrated the reproducibility of our results across independently acquired datasets as a means for establishing statistical validity (Ioannidis et al., 2014; Picciotto, 2018). Indeed, the meta-analysis approach we have taken here allowed us to confirm the robust and reproducible nature of the reported effects. Our findings therefore provide solid evidence to the ongoing debate regarding the role of neighborhood relationships in driving cortical reorganization, and emphasize the need to consider sensorimotor reorganization as a more complex phenomenon than has previously been discussed.

If the extent of overlap between body-part representations does not account for reorganization, what could drive the large-scale sensorimotor reorganization reported by us and others? One possibility is that reorganization is shaped by altered inputs to the deprived cortex, which are associated with compensatory behavior. We have previously characterized the behavioral repertoire of one-handers, and found that these individuals use their residual arm, lips and feet to compensate for the absence of a hand (Hahamy et al., 2017). As previously reported and further extended here, the same body-parts used for compensatory purposes also remap onto the deprived hand regions of both the cerebellum and cerebrum. Importantly, the intact hand, which is not over-used for compensatory purposes (Makin et al., 2013b; Philip and Frey, 2014; Hahamy et al., 2017), does not show remapping into either the cerebellar or cerebral deprived hand regions. While these findings suggest compensatory behavior as a driver for reorganization, it is important to note that so far we were unable to find a correlation between individuals' idiosyncratic compensatory strategies and brain reorganization. Indeed, other studies reported large-scale reorganization that did not reflect compensatory behavioral profiles (Yu et al., 2014; Striem-Amit et al., 2018), though compensatory daily behavior is difficult to quantify comprehensively and reliably.

Similar controversy also exist in reports of reorganization in adulthood following limb amputation, which is most commonly reported as remapping of the residual arm (Kew et al., 1994;

Irlbacher et al., 2002; Raffin et al., 2016) (but see Gagne et al., 2011; Makin et al., 2013b) and mouth (Flor et al., 1995; Elbert et al., 1997; Karl et al., 2001; Lotze et al., 2001; MacIver et al., 2008; Foell et al., 2014), (though see Makin et al., 2013a; Makin et al., 2015; Raffin et al., 2016), both thought to neighbor the hand region (though see Zeharia et al., 2015; Roux et al., 2018; as well as hand and lip regions in Figure 5). Nevertheless, more recent findings reveal remapping of the intact hand representation (which resides in the opposite hemisphere) onto the deprived hand region in adult human amputees (Bogdanov et al., 2012; Makin et al., 2013b; Philip and Frey, 2014). These more recent findings have ascribed intact hand remapping to adaptive reorganization, reflecting the compensatory use of the intact hand by amputees.

Thus, findings across varied sensorimotor-deprived populations raise the possibility that body-part representations that have very little overlap, if any, with the hand region (lips and feet in one-handers, feet in individuals with bilateral congenital limb loss or childhood amputation, and intact hand in amputated adults) can remap onto the deprived hand region, provided that this remapping corresponds with behavioral change. Conversely, representations of body-parts which neighbor the deprived hand region can also show reorganization, even under reduced behavioral pressure (Striem-Amit et al., 2018). Note, however, that this opponent report was based on only 5 participants, and therefore awaits further confirmation.

It should also be noted that the absence of intact hand representation in the missing hand region of one-handers could stem from reasons other than lack of compensatory use of the intact hand. For example, in the current experimental design, the intact hand is the only body-part contralateral to the deprived cerebral hemisphere/ipsilateral to the deprived cerebellar hemisphere (note that movements of the lips and feet were performed bilaterally in this experiment). We therefore cannot exclude the possibility that reorganization in the missing hand area of one-handers is restricted to body-part representations that reside within the deprived hemisphere.

We also cannot exclude the possibility that behavior and brain reorganization may not be directly related. For example, the observed reorganization in one-handers may merely reflect weak normal inputs

from different body-parts to the hand area, which are typically supressed by the main inputs from the hand. These inputs may be simply unmasked in the absence of a hand, and may not necessarily causally support compensatory behaviour (for further discussion see Krakauer and Carmichael, 2017; Makin and Bensmaia, 2017). Taken together, further research is needed to validate the causal origins and consequences of behaviour on the large scale reorganization reported here.

Finally, it may also be conjectured that the reported reorganization is indeed constrained by proximity between body-part representations - not in the cerebellum/cerebrum, but rather in subcortical terminals of the sensorimotor pathway. Consistent with this conjecture, while it has originally been suggested that somatosensory reorganization occurs at the level of the cerebral cortex (Pons et al., 1991; Florence et al., 1998), recent studies in monkeys emphasize the role of subcortical structures, such as the brainstem, in which the layout of somatotopic representations differs from that seen in the cerebral cortex (Jain et al., 2000; Kambi et al., 2014; Chand and Jain, 2015; Liao et al., 2016). For example, Kambi and colleagues (2014) have recently demonstrated that facial reorganization in the deprived cerebral hand region of spinal-cord-injured monkeys is abolished upon inactivation of the deprived cuneate nucleus. The fact that the cuneate nucleus does not normally receive inputs from the face suggests that reorganization seen in the cerebral cortex is likely driven by reorganization at the level of the brainstem (see also Herbert et al., 2015 for a related example of reorganization in the motor cortex). Taken together with our current findings, it is particularly tempting to speculate that the upstream sensorimotor terminal at which reorganization may be initiated would contain a somatotopic layout specifically suitable for supporting the emerging repertoire of compensatory behaviors.

Indeed, our data provide initial evidence for reorganization in the putamen of one-handers, which demonstrates the same pattern of body-part remapping (residual arm, lip and foot) as in the cerebral and cerebellar cortices. Interestingly, it has been demonstrated that representations of the hand, lip and foot, which are distal in the cerebral cortex, neighbor each other in the putamen of the human basal ganglia (Gerardin et al., 2003; Staempfli et al., 2008). These neighboring representations may thus more easily remap to the deprived hand region, and consequently, projections from the putamen hand representation

to its cerebral/cerebellar counterparts would appear as reorganization that is independent of the cerebral/cerebellar somatotopic layout. This hypothesis is particularly appealing since the primary sensorimotor cortex, cerebellum and basal ganglia form a closed-loop, reciprocal circuit, such that each terminal projects to and receives inputs from each other terminal, with varying layouts of somatotopy within each terminal (Nambu, 2011; Dum et al., 2014; Zeharia et al., 2015). As our findings reveal reorganization in all three of these interconnected terminals, it is tempting to conjecture that this reorganization is perhaps initiated by the basal ganglia. However, the results reported in the putamen were only observed in the one dataset, and lacked the spatial resolution to accurately allocate the position of the putamen hand region. These results are therefore not as robust as those we reported in the cerebral and cerebellar cortices. In addition, since our results demonstrate remapping in both primary somatosensory and motor cortices (Figure 5), which have differing upstream hierarchies, this interesting interpretation awaits further confirmation.

Funding

This work was supported by the European Molecular Biology Organization non-stipendiary Long-Term Fellowship (848-2017), Human Frontier Science Program (LT000444/2018), Israeli National Postdoctoral Award Program for Advancing Women in Science, the Israeli Presidential Bursary for outstanding PhD students in brain research and the Boehringer Ingelheim Fonds travel grant to AH. TM was supported by a Sir Henry Dale Fellowship jointly funded by the Wellcome Trust and the Royal Society (grant number 104128/Z/14/Z), and the European Research Council Starting Grant (grant number 715022 — EmbodiedTech).

References

Andoh J, Milde C, Tsao JW, Flor H (2017) Cortical plasticity as a basis of phantom limb pain: Fact or fiction? Neuroscience.

Bogdanov S, Smith J, Frey SH (2012) Former hand territory activity increases after amputation during intact hand movements, but is unaffected by illusory visual feedback. Neurorehabil Neural Repair 26:604-615.

Buckner RL, Krienen FM, Castellanos A, Diaz JC, Yeo BT (2011) The organization of the human cerebellum estimated by intrinsic functional connectivity. J Neurophysiol 106:2322-2345.

Catani M (2017) A little man of some importance. Brain 140:3055-3061.

Chand P, Jain N (2015) Intracortical and Thalamocortical Connections of the Hand and Face Representations in Somatosensory Area 3b of Macaque Monkeys and Effects of Chronic Spinal Cord Injuries. J Neurosci 35:13475-13486.

Dice LR (1945) Measures of the amount of ecologic association between species. Ecology 26:297-302.

Diedrichsen J, Zotow E (2015) Surface-Based Display of Volume-Averaged Cerebellar Imaging Data. PLoS One 10:e0133402.

Dum RP, Bostan AC, Strick PL (2014) 36 Basal Ganglia and Cerebellar Circuits with the Cerebral Cortex. The cognitive neurosciences:419.

Elbert T, Sterr A, Flor H, Rockstroh B, Knecht S, Pantev C, Wienbruch C, Taub E (1997) Input-increase and input-decrease types of cortical reorganization after upper extremity amputation in humans. Exp Brain Res 117:161-164.

Faggin BM, Nguyen KT, Nicolelis MA (1997) Immediate and simultaneous sensory reorganization at cortical and subcortical levels of the somatosensory system. Proc Natl Acad Sci U S A 94:9428-9433.

Fisher R (1948) Questions and answers# 14. The American Statistician 2:30-31.

Fisher RA (1925) Statistical methods for research workers: Genesis Publishing.

Flor H, Elbert T, Knecht S, Wienbruch C, Pantev C, Birbaumer N, Larbig W, Taub E (1995) Phantom-limb pain as a perceptual correlate of cortical reorganization following arm amputation. Nature 375:482-484.

Florence SL, Taub HB, Kaas JH (1998) Large-scale sprouting of cortical connections after peripheral injury in adult macaque monkeys. Science 282:1117-1121.

Foell J, Bekrater-Bodmann R, Diers M, Flor H (2014) Mirror therapy for phantom limb pain: brain changes and the role of body representation. Eur J Pain 18:729-739.

Friston K (2012) Ten ironic rules for non-statistical reviewers. Neuroimage 61:1300-1310.

Gagne M, Hetu S, Reilly KT, Mercier C (2011) The map is not the territory: motor system reorganization in upper limb amputees. Hum Brain Mapp 32:509-519.

Gerardin E, Lehericy S, Pochon JB, Tezenas du Montcel S, Mangin JF, Poupon F, Agid Y, Le Bihan D, Marsault C (2003) Foot, hand, face and eye representation in the human striatum. Cereb Cortex 13:162-169.

Greve DN, Fischl B (2009) Accurate and robust brain image alignment using boundary-based registration. Neuroimage 48:63-72.

Grodd W, Hulsmann E, Lotze M, Wildgruber D, Erb M (2001) Sensorimotor mapping of the human cerebellum: fMRI evidence of somatotopic organization. Hum Brain Mapp 13:55-73.

Haak KV, Marquand AF, Beckmann CF (2017) Connectopic mapping with resting-state fMRI. Neuroimage.

Hahamy A, Behrmann M, Malach R (2015a) The idiosyncratic brain: distortion of spontaneous connectivity patterns in autism spectrum disorder. Nat Neurosci.

Hahamy A, Sotiropoulos SN, Henderson Slater D, Malach R, Johansen-Berg H, Makin TR (2015b) Normalisation of brain connectivity through compensatory behaviour, despite congenital hand absence. eLife 4.

Hahamy A, Macdonald SN, van den Heiligenberg F, Kieliba P, Emir U, Malach R, Johansen-Berg H, Brugger P, Culham JC, Makin TR (2017) Representation of Multiple Body Parts in the Missing-Hand Territory of Congenital One-Handers. Curr Biol 27:1350-1355.

Herbert WJ, Powell K, Buford JA (2015) Evidence for a role of the reticulospinal system in recovery of skilled reaching after cortical stroke: initial results from a model of ischemic cortical injury. Exp Brain Res 233:3231-3251.

Holmes AP, Blair RC, Watson JD, Ford I (1996) Nonparametric analysis of statistic images from functional mapping experiments. J Cereb Blood Flow Metab 16:7-22.

Ioannidis JP, Munafo MR, Fusar-Poli P, Nosek BA, David SP (2014) Publication and other reporting biases in cognitive sciences: detection, prevalence, and prevention. Trends Cogn Sci 18:235-241.

Irlbacher K, Meyer BU, Voss M, Brandt SA, Roricht S (2002) Spatial reorganization of cortical motor output maps of stump muscles in human upper-limb amputees. Neurosci Lett 321:129-132.

Jain N, Florence SL, Qi HX, Kaas JH (2000) Growth of new brainstem connections in adult monkeys with massive sensory loss. Proc Natl Acad Sci U S A 97:5546-5550.

Jain N, Qi HX, Collins CE, Kaas JH (2008) Large-scale reorganization in the somatosensory cortex and thalamus after sensory loss in macaque monkeys. J Neurosci 28:11042-11060.

Jang JH, Jung WH, Choi JS, Choi CH, Kang DH, Shin NY, Hong KS, Kwon JS (2011) Reduced prefrontal functional connectivity in the default mode network is related to greater psychopathology in subjects with high genetic loading for schizophrenia. Schizophr Res 127:58-65.

Jenkinson M, Bannister P, Brady M, Smith S (2002) Improved optimization for the robust and accurate linear registration and motion correction of brain images. Neuroimage 17:825-841.

Kaas JH, Qi HX, Burish MJ, Gharbawie OA, Onifer SM, Massey JM (2008) Cortical and subcortical plasticity in the brains of humans, primates, and rats after damage to sensory afferents in the dorsal columns of the spinal cord. Exp Neurol 209:407-416.

Kambi N, Halder P, Rajan R, Arora V, Chand P, Arora M, Jain N (2014) Large-scale reorganization of the somatosensory cortex following spinal cord injuries is due to brainstem plasticity. Nat Commun 5:3602.

Karl A, Birbaumer N, Lutzenberger W, Cohen LG, Flor H (2001) Reorganization of motor and somatosensory cortex in upper extremity amputees with phantom limb pain. J Neurosci 21:3609-3618.

Kew JJ, Ridding MC, Rothwell JC, Passingham RE, Leigh PN, Sooriakumaran S, Frackowiak RS, Brooks DJ (1994) Reorganization of cortical blood flow and transcranial magnetic stimulation maps in human subjects after upper limb amputation. J Neurophysiol 72:2517-2524.

Kikkert S, Kolasinski J, Jbabdi S, Tracey I, Beckmann CF, Johansen-Berg H, Makin TR (2016) Revealing the neural fingerprints of a missing hand. Elife 5.

Krakauer JW, Carmichael ST (2017) Broken Movement: The Neurobiology of Motor Recovery After Stroke: MIT Press.

Liao CC, Reed JL, Kaas JH, Qi HX (2016) Intracortical connections are altered after long-standing deprivation of dorsal column inputs in the hand region of area 3b in squirrel monkeys. J Comp Neurol 524:1494-1526.

Liptak T (1958) On the combination of independent tests. Magyar Tud Akad Mat Kutato Int Kozl 3:171-197.

Lotze M, Flor H, Grodd W, Larbig W, Birbaumer N (2001) Phantom movements and pain. An fMRI study in upper limb amputees. Brain 124:2268-2277.

MacIver K, Lloyd DM, Kelly S, Roberts N, Nurmikko T (2008) Phantom limb pain, cortical reorganization and the therapeutic effect of mental imagery. Brain 131:2181-2191.

Makin TR, Bensmaia SJ (2017) Stability of Sensory Topographies in Adult Cortex. Trends Cogn Sci.

Makin TR, Scholz J, Henderson Slater D, Johansen-Berg H, Tracey I (2015) Reassessing cortical reorganization in the primary sensorimotor cortex following arm amputation. Brain 138:2140-2146.

Makin TR, Scholz J, Filippini N, Slater DH, Tracey I, Johansen-Berg H (2013a) Phantom pain is associated with preserved structure and function in the former hand area. Nature Communications 4.

Makin TR, Cramer AO, Scholz J, Hahamy A, Slater DH, Tracey I, Johansen-Berg H (2013b) Deprivation-related and use-dependent plasticity go hand in hand. Elife 2.

Manni E, Petrosini L (2004) A century of cerebellar somatotopy: a debated representation. Nat Rev Neurosci 5:241-249.

Margolis DJ, Lutcke H, Schulz K, Haiss F, Weber B, Kugler S, Hasan MT, Helmchen F (2012) Reorganization of cortical population activity imaged throughout long-term sensory deprivation. Nat Neurosci 15:1539-1546.

Masyn K, Nathan P, Little T (2013) The Oxford Handbook of Quantitative Methods, Vol. 2: Statistical Analysis.

Merzenich MM, Jenkins WM (1993) Reorganization of cortical representations of the hand following alterations of skin inputs induced by nerve injury, skin island transfers, and experience. J Hand Ther 6:89-104.

Merzenich MM, Nelson RJ, Stryker MP, Cynader MS, Schoppmann A, Zook JM (1984) Somatosensory cortical map changes following digit amputation in adult monkeys. J Comp Neurol 224:591-605.

Mottolese C, Szathmari A, Beuriat PA, Sirigu A, Desmurget M (2015) Sensorimotor mapping of the human cerebellum during pineal region surgery. Neurochirurgie 61:101-105.

Mottolese C, Richard N, Harquel S, Szathmari A, Sirigu A, Desmurget M (2013) Mapping motor representations in the human cerebellum. Brain 136:330-342.

Nambu A (2011) Somatotopic organization of the primate Basal Ganglia. Front Neuroanat 5:26.

Nichols TE, Holmes AP (2002) Nonparametric permutation tests for functional neuroimaging: a primer with examples. Human brain mapping 15:1-25.

Penfield W, Boldrey E (1937) Somatic motor and sensory representation in the cerebral cortex of man as studied by electrical stimulation. Brain: A journal of neurology.

Penfield W, Rasmussen T (1950) The cerebral cortex of man; a clinical study of localization of function.

Philip BA, Frey SH (2014) Compensatory changes accompanying chronic forced use of the nondominant hand by unilateral amputees. J Neurosci 34:3622-3631.

Picciotto M (2018) Analytical Transparency and Reproducibility in Human Neuroimaging Studies. J Neurosci 38:3375-3376.

Pons TP, Garraghty PE, Ommaya AK, Kaas JH, Taub E, Mishkin M (1991) Massive cortical reorganization after sensory deafferentation in adult macaques. Science 252:1857-1860.

Raffin E, Richard N, Giraux P, Reilly KT (2016) Primary motor cortex changes after amputation correlate with phantom limb pain and the ability to move the phantom limb. Neuroimage 130:134-144.

Roux FE, Djidjeli I, Durand JB (2018) Functional architecture of the somatosensory homunculus detected by electrostimulation. The Journal of physiology 596:941-956.

Smith SM (2002) Fast robust automated brain extraction. Hum Brain Mapp 17:143-155.

Staempfli P, Reischauer C, Jaermann T, Valavanis A, Kollias S, Boesiger P (2008) Combining fMRI and DTI: a framework for exploring the limits of fMRI-guided DTI fiber tracking and for verifying DTI-based fiber tractography results. Neuroimage 39:119-126.

Stoeckel MC, Seitz RJ, Buetefisch CM (2009) Congenitally altered motor experience alters somatotopic organization of human primary motor cortex. Proc Natl Acad Sci U S A 106:2395-2400.

Stouffer SA, Suchman EA, DeVinney LC, Star SA, Williams Jr RM (1949) The American Soldier: Princeton University Press, Princeton.

Striem-Amit E, Vannuscorps G, Caramazza A (2018) Plasticity based on compensatory effector use in the association but not primary sensorimotor cortex of people born without hands. Proc Natl Acad Sci U S A 115:7801-7806.

Wiestler T, McGonigle DJ, Diedrichsen J (2011) Integration of sensory and motor representations of single fingers in the human cerebellum. J Neurophysiol 105:3042-3053.

Yu XJ, He HJ, Zhang QW, Zhao F, Zee CS, Zhang SZ, Gong XY (2014) Somatotopic reorganization of hand representation in bilateral arm amputees with or without special foot movement skill. Brain Res 1546:9-17.

Zeharia N, Hertz U, Flash T, Amedi A (2015) New whole-body sensory-motor gradients revealed using phase-locked analysis and verified using multivoxel pattern analysis and functional connectivity. J Neurosci 35:2845-2859.

Tables

Table 1. Demographic details of individuals with congenital limb-absence included in Dataset2 (Full details of the participants of Dataset1 are available in Hahamy et al., 2015b).

Participant	Age	Gender	Level of limb deficiency	Affected limb	participated in both studies
1	39	Male	below elbow	Left	yes
2	35	Male	below elbow	Right	
3	29	Female	below elbow	Left	
4	58	Male	below elbow	Left	yes
5	37	Female	below elbow	Right	yes
6	52	Female	below elbow	Left	
7	32	Male	below elbow	Left	
8	61	Male	below elbow	Left	
9	42	Female	below elbow	Left	
10	53	Female	below elbow	Right	yes

11	44	Male	below elbow	Left
12	35	Male	below elbow	Right
13	51	Female	below elbow	Left
14	63	Female	below elbow	Right

Table 2. Number of voxels ($(2mm)^3$) and center-of-gravity coordinates of regions of interest.

	# voxels	Coordinates
Intact/dominant hand (cerebellum, Dataset1)	100	21,-51,-21
Deprived/nondominant hand (cerebellum, Dataset1)	100	-21,-52,-21
Intact/dominant hand (cerebellum, Dataset2)	100	21,-51,-22
Deprived/nondominant hand (cerebellum, Dataset2)	100	-20,-51,-24
Intact/dominant hand (cerebrum)	388	38, -22, 56
Deprived/nondominant hand (cerebrum)	388	-38, -22, 56
Intact/dominant putamen	286	26, 4, 0
Deprived/nondominant putamen	321	-26, 4, 0

Table 3. Group-contrast statistics of activation in the hand regions. The number of voxels (#vox), peak intensity (z_{max}) and coordinates of the center of gravity of hand-region activations in the cerebellum and cerebrum are presented for each dataset (rows) and task-condition (columns). Coordinates are based on the MNI 152 brain template.

Brain region	Dataset		Residual arm	Lips	Feet
Cerebellum	1	# vox	-	329	246
		Z_{max}	-	5	3.94
		Coordinates	-	-13,-55,-17	-21,-58,-16
	2	# vox	-	594	623
		Z_{max}	-	4.45	4.03
		Coordinates	-	-17,-59,-21	-21,-57,-22
Cerebrum	1	# vox	244	439	268
		Z_{max}	3.82	4.5	4.11
		Coordinates	46,-20,58	45,-17,54	44,-20,58
	2	# vox	422	411	450
		Z_{max}	5.79	4.24	4.14
		coordinates	49,-20,56	48,-16,54	52,-22,50

Table 4. Group-contrast statistics of increased activation in one-handers compared to controls outside the hand regions. The number of voxels (#vox), peak intensity (z_{max}) and coordinates of the center of gravity of significant activation clusters are presented for each dataset and task-condition. Coordinates are based on the MNI 152 brain template.

Dataset	condition	Region	Region	Region
1	Lips	supracalcarine cortex, 735 voxels, Z_{max} =3.75, (2,-79,13)	Deprived \ nondominant occipital pole, 342 voxels, Z_{max} =4.01, (20,-91,23)	Intact \ dominant parahippocampal gyrus, 217 voxels, Z_{max} =3.9, (-26,-10,-23)
2	Lips	Deprived \ nondominant putamen, 288 voxels, Z_{max} =3.7, (26,-4, -1)	Intact \ dominant parahippocampal gyrus, 187 voxels, Z_{max} =3.83, (-30,-17,-28)	Deprived \ nondominant cerebellar lobule VIIb, 167 voxels, Z_{max} =4, (-7, -78, -48)
	Feet	Intact \ dominant frontal pole, 221 voxels, Z_{max} =4.18, (-27,57,0)	Deprived \ nondominant frontal pole, 177 voxels, Z_{max} =3.65, (29,49,7)	

Table 5. Dataset-specific p-values per brain region and experimental condition. Dataset-specific p-values (rows) are derived from permutation tests for each experimental condition (columns) for both cerebellar and cerebral hand ROIs (top\bottom of table, respectively). Results of dataset 3 were previously reported in Hahamy et al. 2017. Results for the residual arm condition in a subsample of participants from Dataset1 were reported in Makin et al. 2013.

Brain region	Test	Dataset	Residual arm	Lips	Feet	Intact hand
Cerebellum	Group contrasts	1	0.02	0.002	0.04	0.49
		2	0.02	0.004	0.001	0.38
	Group by Hemisphere interaction	1	0.04	0.009	0.11	0.46
		2	0.0008	0.007	<0.001	0.4
Cerebrum	Group contrasts	1	<0.001	0.003	<0.001	0.37
		2	0.03	<0.001	0.004	0.28
		3	<0.001	<0.001	0.04	0.15
	Group by Hemisphere interaction	1	0.03	0.04	<0.001	0.43
		2	0.05	0.02	0.15	0.16
		3	<0.001	0.002	0.23	0.25

Table 6. Assessment of the consistency of results across datasets using additional meta-analysis methods. Results are based on the Stouffer's test (Stouffer et al., 1949) and the weighted Z-test (weights set to the square root of each sample size, Liptak, 1958). Resulting p-values (P_s denotes Stouffer's test and P_z denotes the weighted Z-test, α=0.0125 Bonferroni corrected) are presented for the cerebrum and cerebellum hand regions (rows) and for each experimental condition (columns).

Brain region	**Test**	**Residual arm**		**Lips**		**Feet**		**Intact hand**	
		$\mathbf{P_s}$	$\mathbf{P_z}$	$\mathbf{P_s}$	$\mathbf{P_z}$	$\mathbf{P_s}$	$\mathbf{P_z}$	$\mathbf{P_s}$	$\mathbf{P_z}$
Cerebellum	Group contrasts	0.002	0.002	<0.001	<0.001	<0.001	<0.001	0.41	0.42
	Group by Hemisphere interaction	<0.001	<0.001	<0.001	<0.001	<0.001	0.001	0.4	0.4
Cerebrum	Group contrasts	<0.001	<0.001	<0.001	<0.001	<0.001	<0.001	0.13	0.13
	Group by Hemisphere interaction	<0.001	<0.001	<0.001	<0.001	0.001	<0.001	0.14	0.16

Figures

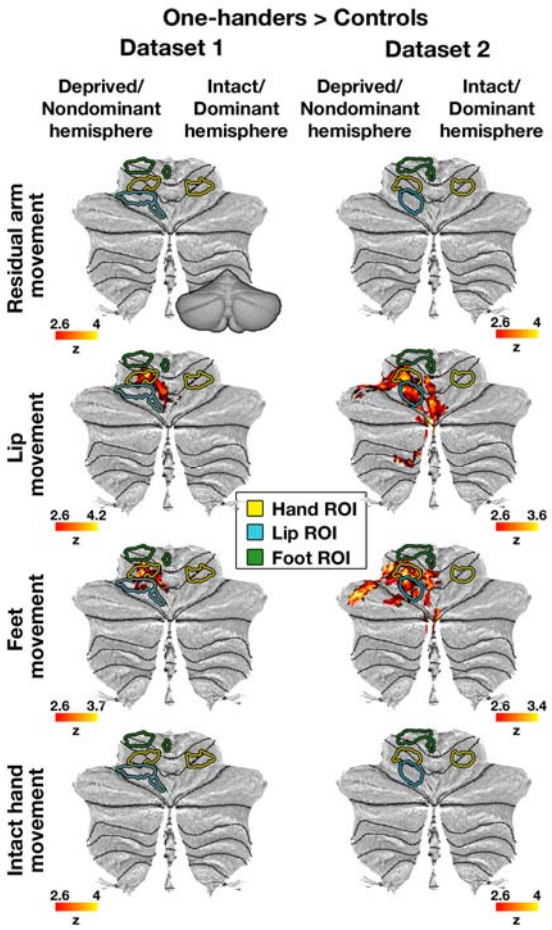

Figure 1. Representation of multiple body-parts in the deprived cerebellar hand region of one-handers: whole-brain analysis. The left/right panels show group contrast maps of Dataset1/Dataset2, respectively, during residual/nondominant arm (one-handers/controls), lips, feet and intact/dominant hand movements, projected onto a flat surface of the cerebellum (see example of an inflated surface on the top left). In the lips and feet (but not residual arm or intact hand) conditions, one-handers showed increased activation compared to controls, centred on the deprived cerebellar hand region. Yellow/blue/green contours indicate the hand/lips/feet ROIs, respectively. Intact/dominant hemisphere, ipsilateral to the intact/dominant hand; deprived/nondominant hemisphere, ipsilateral to missing/nondominant hand. Results of residual arm movements in a subset of participants from Dataset1 were previously reported (Makin et al., 2013b).

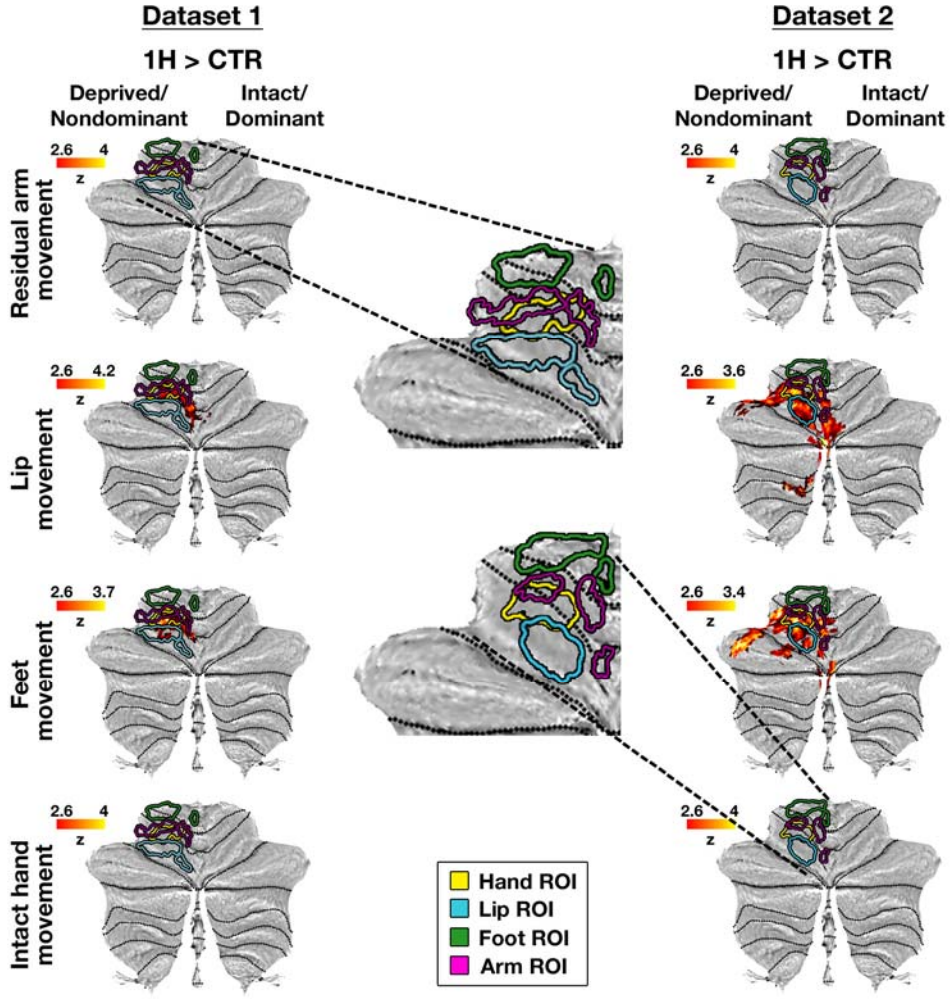

Figure 2. Group-contrast maps in relation to the entire cerebellar homunculus. The left-most and right-most panels presents the same group contrast maps for each dataset and experimental condition as presented in Figure 1, projected onto a flat surface of the cerebellum. Here a pink contour was added to denote the arm ROI, in addition to the yellow/blue/green contours which indicate the hand, lip and foot ROIs, respectively. 1H, one-handers; CTR, controls; Intact/Dominant, hemisphere ipsilateral to the intact/dominant hand; Deprived/Nondominant, hemisphere ipsilateral to missing/nondominant hand.

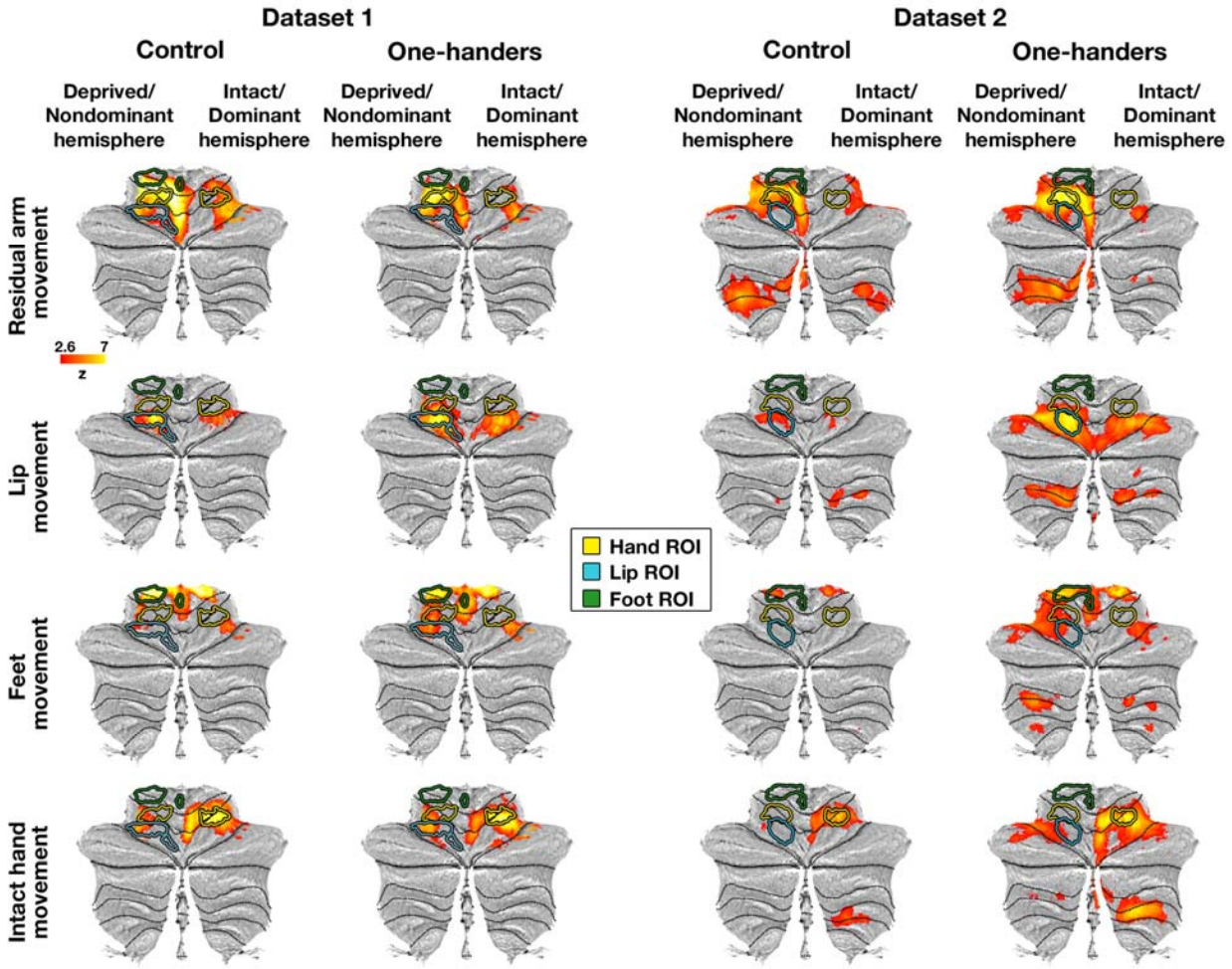

Figure 3. Cerebellar activation group maps. Group maps for each experimental condition vs. a resting baseline (rows) are presented for the control and one-handed groups of each separate dataset (columns). All maps were projected onto a flat surface of the cerebellum, and yellow/blue/green contours indicate the hand/ lip/foot ROIs, respectively. ROIs of each dataset were defined based on the activations of the other dataset to ensure statistical independence in analysis of activations. All maps are presented at an uncorrected threshold of $p<0.01$ to visualize the origin of the group-contrast results presented in Figure 1. Specifically, note the over-activation in the cerebellar deprived hand region of one-handers in the residual arm, lip and foot conditions, compared to controls.

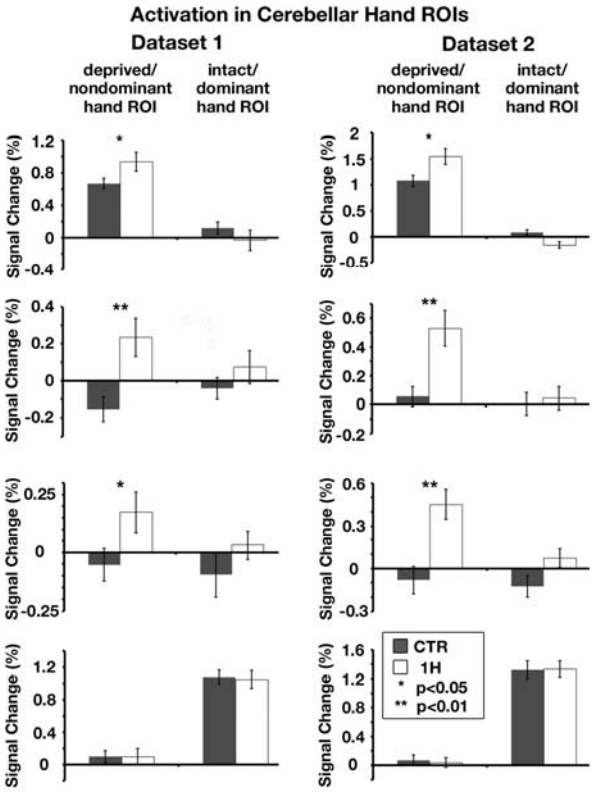

Figure 4. Representation of multiple body-parts in the deprived cerebellar hand region of one-handers: ROI analysis. The left/right panels show activation levels in Dataset1/Dataset2 (respectively) in the bilateral cerebellar hand regions (independently defined for each dataset, ROIs depicted in Figures 1,3), during residual/nondominant arm (one-handers/controls), lips, feet and intact/dominant hand movements. Activation levels in the deprived cerebellar hand region of one-handers (white bars) were greater than activations in the nondominant-hand region of controls (grey bars) in all but the intact hand condition. 1H, one-handers; CTR, controls; intact/dominant hand ROI, ipsilateral to the intact/dominant hand; deprived/nondominant hand ROI, ipsilateral to missing/nondominant hand. Error bars depict SEMs. Results of residual arm movements in a subset of participants from Dataset1 were previously reported (Makin et al., 2013b). Note that the scales of brain activations are not fixed across experimental conditions, to allow a better visual appreciation of the inter-group and inter-hemispheric differences within each condition.

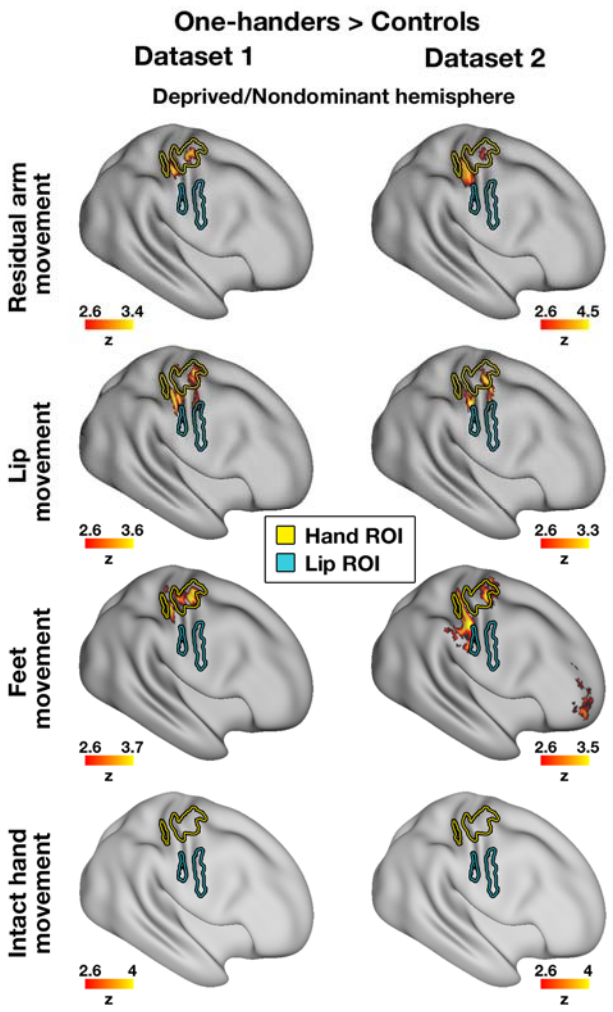

Figure 5. Representation of multiple body-parts in the deprived cerebral hand-region of one-handers: whole-brain analysis. The left/right panels show group contrast maps of Dataset1/Dataset2, respectively, during residual/nondominant arm (one-handers/controls), lips, feet and intact/dominant hand movements, projected onto an inflated surface of a template brain. In each of the arm, lip and feet (but not intact hand) conditions, one-handers showed increased activation compared to controls, centred on the deprived cerebral hand region. Yellow/blue contours indicate the hand/lip ROIs, respectively. Deprived/Nondominant hemisphere, contralateral to missing/nondominant hand. Results of residual arm movements in a subset of participants from Dataset1 were previously reported (Makin et al., 2013b).

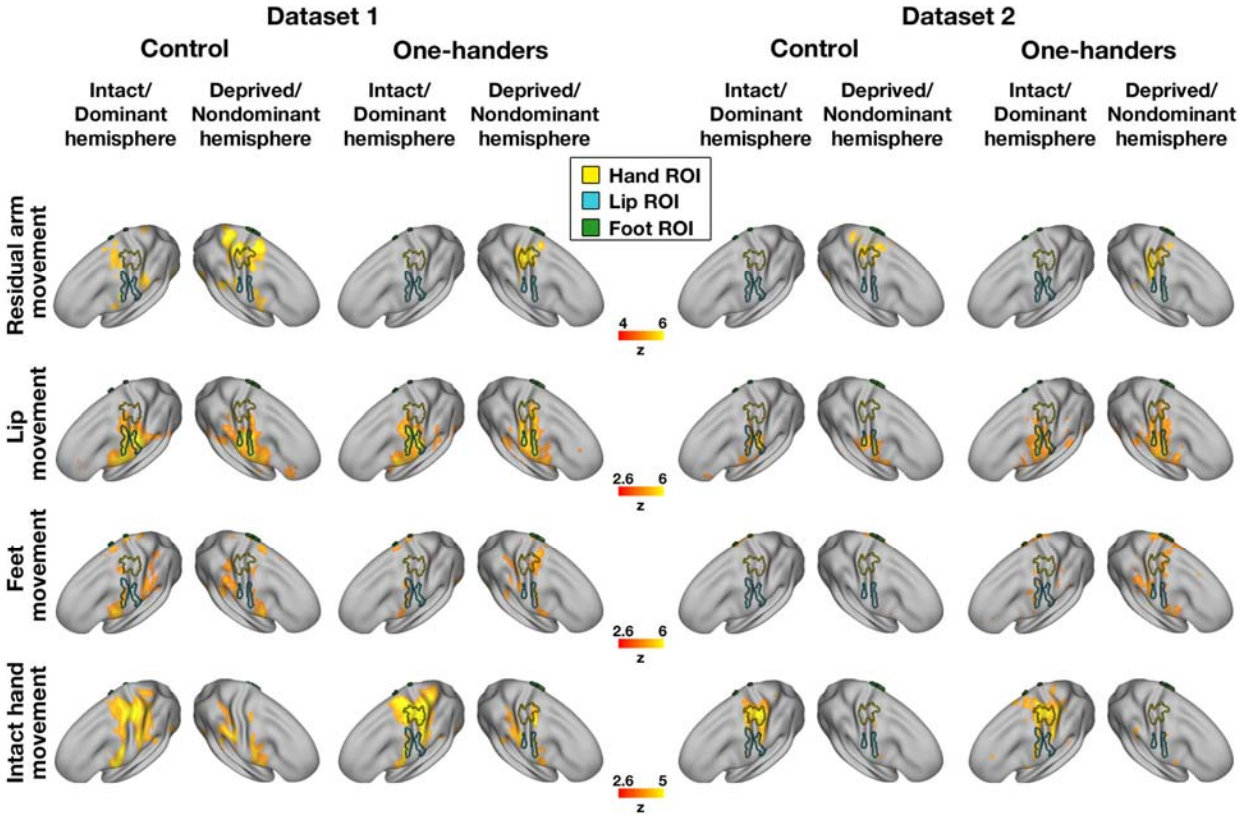

Figure 6. Cerebral activation group maps. Group maps for each experimental condition vs. a resting baseline (rows) are presented for the control and one-handed groups of each separate dataset (columns). All maps were projected onto a flat surface of the cerebral cortex, and yellow/blue/green contours indicate the hand/ lip/foot ROIs, respectively. ROIs were defined based on Dataset3, to ensure full replication of our previously published results in this dataset (Hahamy et al., 2017). All maps are presented at an uncorrected threshold of $p<0.01$ to visualize the origin of the group-contrast results presented in Figure 5. Specifically, note the over-activation in the cerebellar deprived hand region of one-handers in the residual arm, lip and foot conditions, compared to controls. Group maps of Dataset3 can be found at Hahamy et al., 2017.

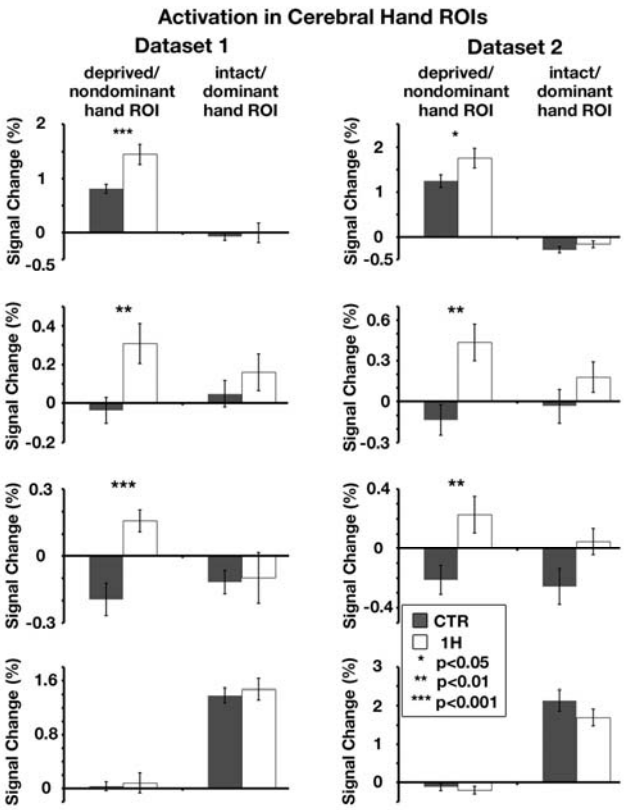

Figure 7. Representation of multiple body-parts in the deprived cerebral hand-region of one-handers: ROI analysis. The left/right panels show activation levels in Dataset1/Dataset2 (respectively) in the bilateral cerebral hand regions (independently defined, ROIs depicted in Figures 5,6), during residual/nondominant arm (one-handers/controls), lips, feet and intact/dominant hand movements. Activation levels in the deprived cerebral hand region of one-handers (white bars) were greater than in the nondominant-hand region of controls (grey bars) in all but the intact hand condition. 1H, one-handers; CTR, controls; intact/dominant hand ROI, contralateral to the intact/dominant hand; deprived/nondominant hand ROI, contralateral to missing/nondominant hand. Error bars depict SEMs. Results of residual arm movements in a subset of participants from Dataset1 were previously reported (Makin et al., 2013b). Note that the scales of brain activations are not fixed across experimental conditions, to allow a better visual appreciation of the inter-group and inter-hemispheric differences within each condition.

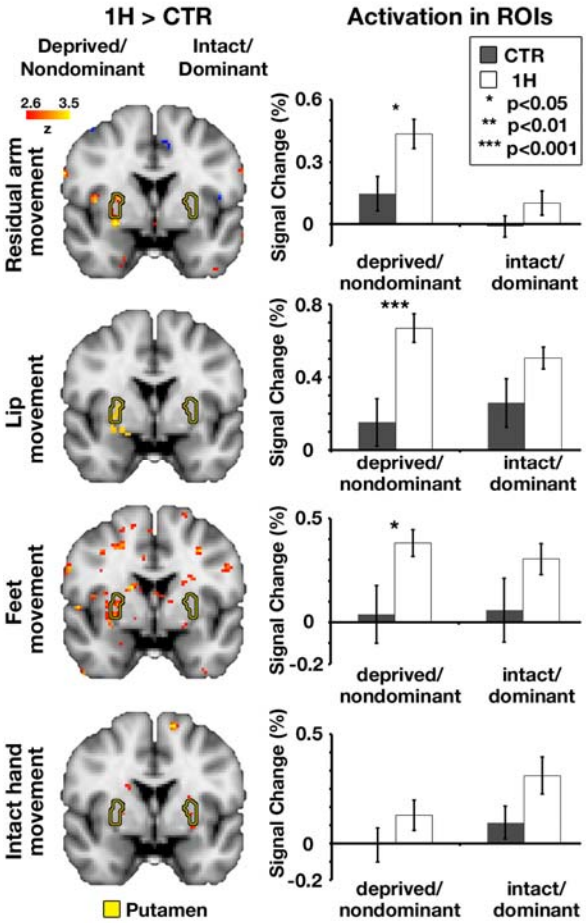

Figure 8. Representation of multiple body-parts in the deprived putamen of one-handers. Left: group contrast maps of Dataset2, during residual/nondominant arm (one-handers/controls), lips, feet and intact/dominant hand movements. In each of the arm, lip and feet (but not intact hand) conditions, one-handers showed increased activation compared to controls, centred on the deprived putamen. Yellow contours indicate the bilateral putamen nuclei. Maps of the residual arm, feet and intact hand conditions are presented at an uncorrected threshold of $p<0.01$. Right: activation levels in Dataset2 in the bilateral putamen nuclei, during each of the experimental conditions. Activation levels in the deprived putamen of one-handers (white bars) were greater than in the nondominant putamen of controls (grey bars) in all but the intact hand condition. 1H, one-handers; CTR, controls; intact/dominant, contralateral to the intact/dominant hand; deprived/nondominant, contralateral to missing/nondominant hand. Error bars depict SEMs.

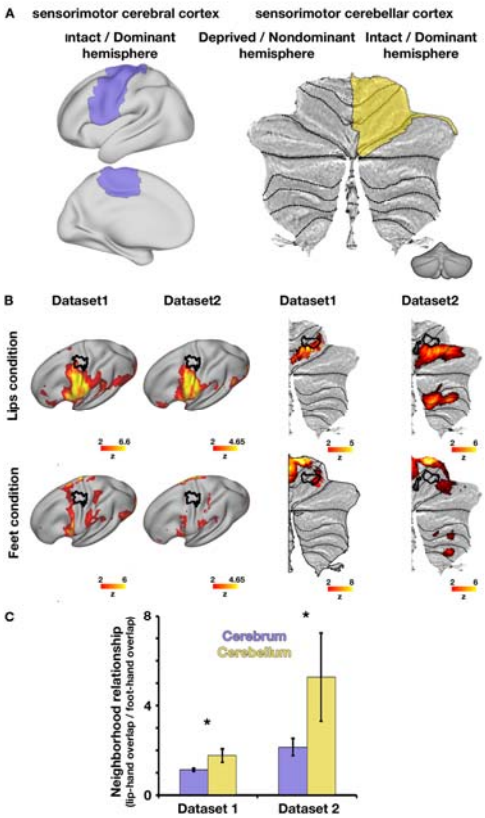

Figure 9. Different overlap relationships of body-part representations between the cerebrum and cerebellum. (A) Sensorimotor masks used to estimate overlap relationships between body-part representations in the intact/dominant cerebral hemisphere (left, marked in purple over an inflated cortical surface) and intact/dominant cerebellar hemisphere (right, marked in yellow over a flattened cerebellar surface). An example of an inflated cerebellar surface is presented on the bottom right of the flat cerebellar surface. Note that the "intact/dominant" cerebral hemisphere is contralateral to the intact/dominant hand (in controls/one-handers, respectively) and the "intact/dominant" cerebellar hemisphere is ipsilateral to the intact/dominant hand. (B) Averaged maps across all participants of each dataset (columns) in the lips (top row) and feet (bottom row) condition, projected onto surfaces of the intact/dominant cerebral (left) and cerebellar (right) hemispheres. Independent ROIs of the intact/dominant hand are depicted in black contours on these same surfaces. Cerebral ROI is taken from Hahamy et al., 2017; cerebellar ROIs were defined as the top 100 voxels activated by intact hand

movements across all participants of one dataset, and presented on the other dataset. These ROIs are presented for illustration purposes alone, and were not used in our statistical analysis of neighborhood relationships, which does not rely on ROIs (see Materials and Methods). (C) Overlap between (i) hand and lip representations and (ii) hand and foot representations were estimated for each participant using the Dice coefficient (see Materials and Methods). The relationship between these overlapping representations was calculated as the ratio between lip-hand overlap and foot-hand overlap (y-axis), which was calculated separately for the cerebrum (purple bars) and cerebellum (yellow bars) within each separate dataset. As evident in both datasets, the levels of overlap between hand-lip and hand-foot representations are less similar in the cerebellum compared to the cerebral cortex (cerebellar ratios>cerebral ratios), demonstrating different somatotopic layout of body-part representations between the cerebral and cerebellar cortices.